Toxicology Letters 368 (2022) 33–46

Contents lists available at ScienceDirect

Toxicology Letters

journal homepage: www.journals.elsevier.com/toxicology-letters

In vitro/in silico prediction of drug induced steatosis in relation to oral doses and blood concentrations by the Nile Red assay

Tim Brecklinghaus [a,*,1], Wiebke Albrecht [a,1], Julia Duda [b,1], Franziska Kappenberg [b], Lisa Gründler [a], Karolina Edlund [a], Rosemarie Marchan [a], Ahmed Ghallab [a,c], Cristina Cadenas [a], Adrian Rieck [a], Nachiket Vartak [a], Laia Tolosa [d], José V. Castell [d,e], Iain Gardner [f], Emina Halilbasic [g], Michael Trauner [g], Anett Ullrich [h], Anja Zeigerer [i,j,m], Özlem Demirci Turgunbayer [a,k], Georg Damm [l], Daniel Seehofer [l], Jörg Rahnenführer [b,2], Jan G. Hengstler [a,**,2]

[a] Leibniz Research Centre for Working Environment and Human Factors at the Technical University of Dortmund (IfADo), Ardeystrasse 67, 44139 Dortmund, Germany
[b] Department of Statistics, TU Dortmund University, Vogelpothsweg 87, 44227, Dortmund, Germany
[c] Department of Forensic Medicine and Toxicology, Faculty of Veterinary Medicine, South Valley University, 83523 Qena, Egypt
[d] Experimental Hepatology Unit, Health Research Institute La Fe, Valencia, Spain
[e] Biochemistry Department, University of Valencia and CIBEREHD
[f] Simcyp (A Certara Company), Sheffield, UK
[g] Hans Popper Laboratory of Molecular Hepatology, Division of Gastroenterology and Hepatology, Department of Internal Medicine III, Medical University of Vienna, Vienna, Austria
[h] Primacyt Cell Culture Technology GmbH, Schwerin, Germany
[i] Institute for Diabetes and Cancer, Helmholtz Center Munich, 85764 Neuherberg, Germany
[j] German Center for Diabetes Research (DZD), 85764 Neuherberg, Germany
[k] Department of Biology, Faculty of Science, Dicle University, 21280, Diyarbakır, Turkey
[l] Department of Hepatobiliary Surgery and Visceral Transplantation, University of Leipzig, 04103 Leipzig, Germany
[m] Joint Heidelberg-IDC Translational Diabetes Program, Inner Medicine 1, Heidelberg University Hospital, Heidelberg, Germany

ARTICLE INFO

Editor: Dr. Angela Mally

Keywords:
Steatosis
DILI
Alternative methods
NAFLD
Lipid droplets

ABSTRACT

The accumulation of lipid droplets in hepatocytes is a key feature of drug-induced liver injury (DILI) and can be induced by a subset of hepatotoxic compounds. In the present study, we optimized and evaluated an in vitro technique based on the fluorescent dye Nile Red, further named Nile Red assay to quantify lipid droplets induced by the exposure to chemicals. The Nile Red assay and a cytotoxicity test (CTB assay) were then performed on cells exposed concentration-dependently to 60 different compounds. Of these, 31 were known to induce hepatotoxicity in humans, and 13 were reported to also cause steatosis. In order to compare in vivo relevant blood concentrations, pharmacokinetic models were established for all compounds to simulate the maximal blood concentrations (C_{max}) at therapeutic doses. The results showed that several hepatotoxic compounds induced an increase in lipid droplets at sub-cytotoxic concentrations. To compare how well (1) the cytotoxicity test alone, (2) the Nile Red assay alone, and (3) the combination of the cytotoxicity test and the Nile Red assay (based on the lower EC_{10} of both assays) allow the differentiation between hepatotoxic and non-hepatotoxic compounds, a previously established performance metric, the Toxicity Separation Index (TSI) was calculated. In addition, the Toxicity Estimation Index (TEI) was calculated to determine how well blood concentrations that cause an increased DILI risk can be estimated for hepatotoxic compounds. Our findings indicate that the combination of both assays improved the TSI and TEI compared to each assay alone. In conclusion, the study demonstrates that inclusion of the Nile Red assay into in vitro test batteries may improve the prediction of DILI compounds.

* Corresponding author.
** Correspondence to: IfADo, Ardeystrasse 67, 44139 Dortmund,x Germany.
E-mail addresses: brecklinghaus@ifado.de (T. Brecklinghaus), hengstler@ifado.de (J.G. Hengstler).
[1] Shared first authorship
[2] Shared senior authorship

https://doi.org/10.1016/j.toxlet.2022.08.006
Received 30 March 2022; Received in revised form 1 August 2022; Accepted 9 August 2022
Available online 10 August 2022

1. Introduction

Recently, an in vitro/in silico method that predicts the risk of human drug-induced liver injury (DILI) in relation to oral doses and blood concentrations was established (Albrecht et al., 2019). This method allows for extrapolation from the lowest concentration that causes a positive test result in vitro to the blood concentrations in vivo, e.g., the plasma peak concentration (C_{max}) that leads to an increased DILI risk. To assess the quality of the in vitro to in vivo extrapolation, two quantitative metrics were introduced, the Toxicity Separation Index (TSI) and the Toxicity Estimation Index (TEI). The TSI quantifies how well the method differentiates between hepatotoxic and non-hepatotoxic compounds for a specific set of substances, while the TEI quantifies how well blood concentrations that lead to an increased DILI risk in vivo can be estimated for hepatotoxic compounds.

Hepatocyte death is a key event often observed in many forms of human hepatotoxicity (Leist et al., 2017). Therefore, cytotoxicity in cultured human hepatocytes was initially used by us and other groups as an in vitro readout for extrapolation to human DILI (Albrecht et al., 2019; Khetani et al., 2013; Proctor et al., 2017; Vorrink et al., 2018). However, hepatotoxicity may also be caused if drugs compromise specific liver functions without immediate cytotoxicity, although hepatocyte death may occur later as a secondary event. Examples include obstructions in the biliary flux (Ghallab et al., 2019; Vartak et al., 2016), inhibition of bile acid export carriers (Dawson et al., 2012; Padda et al., 2011), activation of immune cells (Gerussi et al., 2021; Holland et al., 2022), transformation of stellate cells to myofibroblasts (Ghallab et al., 2019; Hudert et al., 2019), increased production and reduced removal of extracellular matrix (Mohs et al., 2021; Winkler et al., 2020), altered FXR (Matsubara et al., 2013; Schneider et al., 2021) or inflammation-associated (Campos et al., 2020) signaling, and the accumulation of lipid droplets in hepatocytes (Ghallab et al., 2021; Scorletti and Carr, 2022). It remains to be studied if in vitro tests that recapitulate these functions will improve the TSI and TEI for the prediction of DILI. In this respect, a recent pilot study used an in vitro test that detects the inhibition of drug export carriers on the apical membrane of hepatocytes, which secrete bile acids into bile canaliculi (Brecklinghaus et al., 2022). For some compounds, the effective concentration (EC_{10}) for export inhibition was substantially lower than the EC_{10} of cytotoxicity. When the lower EC_{10} of either cytotoxicity or export inhibition was used, better TSI and TEI were obtained compared to the analysis of cytotoxicity alone. These positive findings prompted us to further develop in vitro tests to measure liver functions known to be compromised by specific hepatotoxic compounds and to integrate them into our test battery.

It is well-known that many hepatotoxic compounds induce steatosis at sub-cytotoxic concentrations (Donato et al., 2012; Pessayre et al., 2012). Previously, several techniques have been reported to induce lipid droplet formation in primary hepatocytes and hepatocyte cell lines (Donato et al., 2006; Malhi et al., 2006; Müller and Sturla, 2019). For example, oleic acid or a combination of oleic acid and palmitic acid added to the culture medium successfully resulted in lipid droplets in cells (Barbero-Becerra et al., 2015; Gómez-Lechón et al., 2007; Kostrzewski et al., 2017). In the present study, we optimized an in vitro test that detects if a test compound causes an accumulation of lipid droplets, and studied if this assay improves the TSI and TEI compared to the analysis of cytotoxicity alone.

2. Materials and methods

2.1. Test compounds

The supplier and chemical information of the test compounds are listed in Supplement 1. Furthermore, information on hepatotoxicity and case reports of steatosis is also given.

2.2. Cultivation of primary human hepatocytes

Cryopreserved primary human hepatocytes (PHH) were purchased from BioIVT and Lonza. The donor characteristics are given in Supplement 1. Cells were cultivated according to a previously published standard operating procedure (SOP) (Gu et al., 2018). In brief, PHH were thawed and suspended in phenol red free William's E media (P04–29510, PAN-Biotech, Aidenbach, Germany) supplemented with 2 mM glutamine (P04–82100, PAN-Biotech, Aidenbach, Germany), 100 nM dexamethasone (D4902, Sigma Aldrich, Darmstadt, Germany), 10 ng/ml Insulin-Transferrin-Selenium (ITS), (13146, Sigma Aldrich, Darmstadt, Germany), 100 U/ml penicillin and 0.1 mg/ml streptomycin (P06–07100, PAN-Biotech, Aidenbach, Germany), 10 µg/ml gentamicin (P06–03021, PAN-Biotech, Aidenbach, Germany) and 10% (v/v) SeraPlus (3702-P103009, PAN-Biotech, Aidenbach, Germany). After counting and diluting, 50,000 or 200,000 viable cells were seeded onto collagen coated black 96-well plates (655986, Greiner Bio-One, Kremsmünster, Austria) or 4-well IBIDI chambers (80426, Ibidi, Gräfelfing, Germany). To avoid edge effects, the outer wells of the 96-well plate were filled with culture medium only. After 3–4 h of attachment, the medium was changed to serum free William's E medium with the aforementioned supplements and cells were cultured under standard conditions for 16–20 h (37 °C in a humidified atmosphere with 5% CO_2).

2.3. Cytotoxicity in primary human hepatocytes (CTB assay)

The CTB cytotoxicity test was performed as described previously (Gu et al., 2018). In brief, the next day after seeding, the cells were incubated with 200 µl of the indicated test compound concentrations and a corresponding solvent control for 48 h. After incubation, the cells were washed three times and the CellTiter-Blue® Cell Viability Assay (G8081, Promega, Madison, Wisconsin, USA) was performed according to the manufacturer's instructions. Fluorescence was detected with the Tecan Infinite 200Pro fluorescence plate reader (Tecan Trading AG, Switzerland) and the corresponding software, Tecan i-control 2.0.10.0 (λ_{ex} = 540 nm, λ_{em} = 594 nm). Each experiment was performed using hepatocytes from at least three different human donors, each with 3–4 technical replicates. The raw data, processed data and corresponding concentration-response curves are given in Supplement 2 and 3.

2.4. Cultivation of HepG2 cells

Cultivation of HepG2 cells was performed as previously published (Albrecht et al., 2019). HepG2 cells were purchased from ATCC LGC Standards (HB-8065) and cultivated in Dulbecco's Modified Eagle's Medium (P04–04500, PAN Biotech GmbH, Aidenbach, Germany) containing 4.5 g/l glucose, 1% penicillin/streptomycin mixture (P06–07100, PAN Biotech GmbH, Aidenbach, Germany), and 10% heat-inactivated FBS (3702-P103009, PAN Biotech GmbH, Aidenbach, Germany). The cells were maintained in conventional T75 cell culture flasks and kept at 37 °C with constant humidity and 5% CO_2 content. The medium was changed every 2–3 days. Cells were sub-cultured or plated for experiments when they reached 80–90% confluency.

2.5. Free fatty acid (FFA) mix

Free fatty acids were added to Dulbecco's Modified Eagle's Medium (P04–04500, PAN Biotech GmbH, Aidenbach, Germany) containing 4.5 g/l glucose, 1% penicillin/streptomycin mixture (P06–07100, PAN Biotech GmbH, Aidenbach, Germany), and 10% heat-inactivated FBS (3702-P103009, PAN Biotech GmbH, Aidenbach, Germany) in a molar ratio of 1:2 for palmitic acid (P9767, Sigma-Aldrich) and oleic acid (07501, Sigma-Aldrich), respectively.

2.6. Lipid droplet formation in HepG2 cells (Nile Red assay)

For a detailed standard operating procedure (SOP) see Supplement 4. Briefly, 15,000 cells/well were seeded onto collagen coated black 96-well plates (655986, Greiner Bio-One, Kremsmünster, Austria). 24 h after seeding, the cells were incubated with 200 µl of the corresponding test compound and 62 µM free fatty acid mix for 48 h. Afterwards, the cells were washed three times with phosphate buffered saline (PBS) and stained with AdipoRed Assay Reagent™ (PT-7009, Lonza, Basel, Switzerland), (1:40) and Hoechst 33342 (H3570, Thermo Fisher Scientific, Waltham, MA, USA), (1:1000) diluted in PBS. Fluorescence was measured with the Tecan Infinite 200Pro (Tecan Trading AG, Switzerland) fluorescence plate reader and the corresponding software, Tecan i-control 2.0.10.0 with $\lambda_{em/ex}$ of 485/572 nm and 340/460 nm for Nile Red and Hoechst 33342, respectively. Wells with fluorophore but without cells were used for background subtraction and the Nile Red signal was normalized to the Hoechst signal. Three independent biological replicates were performed per experiment with 4 technical replicates. The raw data, processed data and corresponding concentration-response curves are given in Supplement 2 and 3.

2.7. Analysis of the influence of the free fatty acid mixture

To study the effect of increasing fatty acid concentrations on mitochondrial membrane potential and cell count, cells were exposed to FFA for 24 h, 48 h and 72 h and subsequently stained for 10 min with tetramethylrhodamine ethyl ester (TMRE) (T669, Thermo Fisher Scientific, Waltham, MA, USA) and Hoechst (H3570, Thermo Fisher Scientific, Waltham, MA, USA) at room temperature in the dark. Therefore, 200 µl staining solution (200 µl PBS + 0.2 µl 16.2 mM Hoechst solution + 0.1 µl 2 mM TMRE stock) was transferred to each well and subsequently fluorescence was measured with a plate reader Tecan Infinite 200Pro (Tecan Trading AG, Switzerland) and the corresponding software Tecan i-control 2.0.10.0 with excitation wavelengths of 545 nm and 340 nm, and emission of 584 nm and 460 nm emission for TMRE and Hoechst 33342, respectively. Wells with staining solution but without cells served as background control.

To investigate the cytotoxic effect of the FFA mixture on HepG2 cells, the CellTiter-Blue® Cell Viability Assay (G8081, Promega, Madison, Wisconsin, USA) was performed according to the manufacturer's instructions. Fluorescence was measured using the Tecan Infinite 200Pro fluorescence plate reader (Tecan Trading AG, Switzerland) and corresponding software Tecan i-control 2.0.10.0 (λ_{ex} = 540 nm, λ_{em} = 594 nm).

2.8. Fluorescence microscopy

In order to microscopically observe lipid droplet formation, HepG2 cells and PHH were seeded onto collagen coated 4-well IBIDI chambers (80426, Ibidi, Gräfelfing, Germany) as described priviously (Albrecht et al., 2019; Gu et al., 2018). 24 h after seeding, lipid droplet formation was induced by the addition of increasing concentrations (62 µM, 124 µM and 248 µM) of the free fatty acid mix. Subsequently the cells were stained with AdipoRed Assay Reagent™ (Lonza; PT-7009) and Hoechst 33342 (H3570, Thermo Fisher Scientific, Waltham, MA, USA). Images were taken on a Zeiss LSM880 confocal microscope (Zeiss, Oberkochen, Germany) with the corresponding software and a C-Apochromat 63 × /1.2 water immersion objective. Image acquisition was performed with a 488 nm Argon laser and detection bands set to 560–615 nm for Nile Red fluorescence and 405 nm excitation and detection bands set to 421–479 nm for Hoechst.

2.9. Statistical analyses

Statistical analyses were performed with GraphPad Prism Version 9 (GraphPad Software, Inc) and with R, version 4.0.5: (R Core Team, 2021), using the R-packages *DoseFinding,* version 0.9–17 (CRAN - Package DoseFinding, 2019) and *drc,* version 3.0–1 (Ritz et al., 2015). The R package *pROC* was used to calculate the TSI (Robin et al., 2011).

2.9.1. Curve fitting and calculation of EC values of cytotoxicity data

Cytotoxicity data was analyzed as described before (Albrecht et al., 2019; Brecklinghaus et al., 2022). In brief, three different models (a four-parameter log-logistic model (4pLL), a Brain-Cousens model (Brain and Cousens, 1989), and a flat profile) were fitted to the data. Then, the Akaike Information Criterion (AIC) (Akaike, 2011) was calculated for each model, and the model with lowest AIC was selected for normalization in order to obtain a response corresponding to 100% viability at the control and final curve fitting. EC values were calculated only for the curves with the following two properties: The mean response value at the highest tested concentration of the respective compound, $conc_{max}$, was smaller than 90% after normalization and the goodness-of-fit was larger than 0.55. For curves that did not have these properties, EC values were replaced with a so called penalty, defined as $conc_{max} \times 5$. Compound-wise EC-values across all donors were calculated using the minimum, median and maximum. When cryopreserved hepatocytes from individual donors were assessed twice, both resulting EC values were included with weight 0.5 for the calculation of the minimum, median and maximum across all donors. For a detailed overview of the raw and processed data, see Supplement 2 and 3.

2.9.2. Curve fitting and calculation of EC values for the Nile Red assay

Steatosis data was analyzed as described before (Brecklinghaus et al., 2022). In brief, for normalization the replicates of the control values were averaged for each biological replicate. Fluorescence values of all replicates were divided by these control values and multiplied by 100 to obtain percentages. The data was fitted using MCP-Mod (Multiple Comparison Procedure and Modeling), a two-step modelling approach that accounts for model uncertainty (Bretz et al., 2005). In the MCP-step, each concentration-response curve was tested for a possible compound effect, considering different candidate curves. Precisely, a multivariate two-sided contrast t-test was used to test if any of the candidate curves matched the concentration-dependent compound effect. Implicitly, a family wise error rate of $\alpha = 0.05$ is not exceeded to adjust for multiple testing. In the Mod-step, either one model was selected according to the AIC (if p-value < 0.05) or, if no model passed (if p-value ≥ 0.05), a flat concentration-response profile was assumed. The selected model was fitted to the data and for comparability the curves were shifted such that the response at concentration 0 is at 100%. EC_x values were calculated as the lowest concentration where the curve reaches a response of (100+x)%.

To obtain a single EC_x value per compound, the median EC_x values of the three biological replicates was calculated per compound. Alternatively, the minimum and maximum was calculated. Only for analyses where the Nile Red assay-based EC_x values alone were considered, missing EC_x values were replaced by the penalty. When combining Nile Red assay-based EC_x values and CTB assay-based EC_x values, the compound-wise minimum of the two EC_x values was always used and only the CTB assay-based EC_x values were replaced by the penalty in the case of missing values. For a detailed overview of the raw and processed data, see Supplement 2.

2.9.3. Calculation of toxicity separation and estimation indices

Toxicity Separation Index (TSI) and Toxicity Estimation Index (TEI) were calculated as described before (Albrecht et al., 2019; Brecklinghaus et al., 2022). TSI and TEI calculation were based on the in vitro alert concentration (e.g. EC_{10} of the CTB assay) and the in vivo value for the C_{max} for each test compound, as described in detail in (Albrecht et al., 2019). In brief, TSI is derived by calculating for each compound $\log_{10}(C_{max})$-$\log_{10}(EC_{10})$ for all compounds, then sorting the differences in ascending order, selecting a cutoff value in each interval defined by two consecutive differences, and for each cutoff value predicting the

toxicity status of each compound. By comparison of the predicted and the true toxicity status, sensitivity and 1-specificity can be calculated and plotted for each cutoff value. The TSI is calculated as the area under the resulting ROC curve (AUC).

Including only the hepatotoxic compounds, TEI is calculated as:

$$\mathrm{TEI} = 1 - \frac{1}{5} \frac{\sum_{i=1}^{n} \mathbb{1}_{toxic}(i)\mathbb{1}_{x(i)>y(i)}\left|\log_{10}\left(\frac{y(i)}{x(i)}\right)\right|}{\sum_{i=1}^{n} \mathbb{1}_{toxic}(i)}$$

where i = 1,…,n represent the considered compounds, x(i) and y(i) the corresponding in vitro and the in vivo value of compound i and $\mathbb{1}_{(condition)}(i)$ is the indicator function which attains the value 1 if the condition is fulfilled by the compound i, and 0 otherwise.

2.10. Simulation of pharmacokinetics

To calculate C_{max} for each test compound, a physiologically based pharmacokinetic (PBPK) model was constructed as described before (Albrecht et al., 2019) using the Simcyp Simulator (Version 19 and 20; SimCyp, Sheffield, UK). Acetaminophen (APAP) and ethanol (EtOH) however are unique examples, because for both substances there are exposure scenarios where high doses lead to increased risk of hepatotoxicity, as well as exposure scenarios where low doses do not cause an increased risk. All treatment regimens of the analyzed substances and input parameters of the pharmacokinetic simulations are given in Supplement 5.

2.11. Patients

Liver tissue biopsies were acquired from adult patients with NAFLD from the Medical University of Vienna. Based on fibrosis stage, the patients were divided into 5 groups from stage 0 (F0) to stage 4 (F4). The study was conducted in accordance with the ethical guidelines of the 1975 Helsinki Declaration and was approved by the local ethics committee.

2.12. Induction of NAFLD in mice

To induce NAFLD in mice, a model of Western-style diet feeding was used as previously described (Ghallab et al., 2021). Briefly, male C57Bl6/n mice (Janvier Labs, France), 8–10-week-old were fed ad libitum on a high fat high carbohydrate diet (D09100301; Research Diets, USA) up to 30 weeks. Control mice were fed ad libitum on a standard diet (V1534–000; Ssniff, Germany). The experiment was approved by the local animal welfare committee (LANUV, North Rhine-Westphalia, Germany; application number: 81–02. 04. 2020. A304). Liver tissue samples were collected time-dependently, fixed in 4% paraformaldehyde, and embedded in paraffin for histopathology and immunohistochemistry analysis.

2.13. Histopathology and immunohistochemistry

Hematoxylin and eosin (H&E) and immunohistochemistry analysis of macrophages in the mouse and the patient samples were performed in 4-μm-thick paraffin liver tissue sections using an autostainer (Discovery Ultra Automated Slide Preparation System; Roche, Germany), as previously described (Ghallab et al., 2022). Primary antibodies against human CD68 (M0876; Agilent, USA) and mouse F4/80 (MCA497; Bio-Rad, Germany) were used for detecting macrophages in human and mice, respectively.

3. Results

3.1. Lipid droplet formation in cultured cells compared to hepatocytes in vivo

In order to induce lipid droplet formation, we exposed cultured primary human hepatocytes (PHH) and the hepatocellular carcinoma cell line, HepG2 to a combination of oleic acid and palmitic acid in the ratio 2:1 for 24 h and 48 h, as previously reported (Gómez-Lechón et al., 2007). The red fluorophore, Nile Red (Greenspan et al., 1985) was then used to visualize the lipid droplets in living cells. Our results reveal that adding the oleic and palmitic acid mixture to the culture medium at concentrations of 62, 124 and 248 μM caused a concentration dependent increase in lipid droplets (Fig. 1), as determined by the increasing red fluorescence signal. Furthermore, lipid droplet formation was similar in both cell types tested.

Acknowledging that the in vivo situation is more complex than in vitro model systems, we wanted to compare in vitro-induced lipid droplets in hepatocytes to lipid droplets formed in humans and mouse livers. Thus, we used formalin-fixed paraffin embedded liver tissue from NAFLD patients with different fibrosis stages (Holland et al., 2022), and mice fed a lipid rich hypercaloric diet for up to 30 weeks (Ghallab et al., 2021). One observed difference is lipid size where the diameter of the largest lipid droplets was greater in both human and mouse livers (Fig. 2) compared to the largest droplets formed in vitro (Fig. 1). In addition, lipid droplets are zonated in vivo, which is not recapitulated under standard culture conditions. Here, we observed that very large lipid droplets (macrovesicular steatosis) predominantly localized to the pericentral lobular zone in humans, and in the midzonal to periportal region in mice (Fig. 2). A further difference is the influence of the immune system which is absent in vitro; whereas in vivo, we observed that lipid droplets were surrounded by F4/80-positive macrophages (Fig. 2), which are known to play a key role in the induction of liver damage (Ghallab et al., 2021).

Despite the limitations of the in vitro system which lacks the complexity of the in vivo environment, our results nevertheless confirm previous findings (Barbero-Becerra et al., 2015; Gómez-Lechón et al., 2007; Kostrzewski et al., 2017), showing that like hepatocytes in livers, both primary human hepatocytes and HepG2 cells maintain the ability to produce lipid droplets, and may therefore serve as appropriate tools to identify steatogenic drugs.

Since the HepG2 cell line has often been described as a useful cell system for the detection of lipid droplet accumulation (Cui et al., 2010; Gómez-Lechón et al., 2007; Müller and Sturla, 2019; Tolosa et al., 2017), and we observed comparable concentration-dependent lipid droplet accumulation between the PHHs and HepG2 cells (Fig. 1), all further experiments were performed with the HepG2 cell line because it is easier to handle and more cost efficient. Limitations of this selection are addressed in the discussion.

3.2. Establishment of culture conditions to test the influence of chemicals on lipid droplet formation

To test the influence of chemicals on lipid droplet formation, we aimed to establish conditions where oleic and palmitic acid induce a mild increase in lipid droplets, but cytotoxic effects are absent or mild. We hypothesized that an influence of test compounds on lipid droplets should be detectable under such conditions. Therefore, we incubated HepG2 cells for 48 h with a fatty acid mix ranging from 62 to 992 μM (sum concentration of oleic and palmitic acid in a ratio 2:1). The Nile Red fluorescence increased from 62 to 248 μM, followed by a decrease at higher concentrations (Fig. 3A). Mitochondrial activity (TMRE) and intensity of the nuclear stain (Hoechst) decreased at 496 μM, while cytotoxicity measured with the CTB assay increased already at 62 μM (Fig. 3B). Testing different incubation periods with the fatty acid mix (24, 48 and 72 h) revealed that incubation time had no major influence

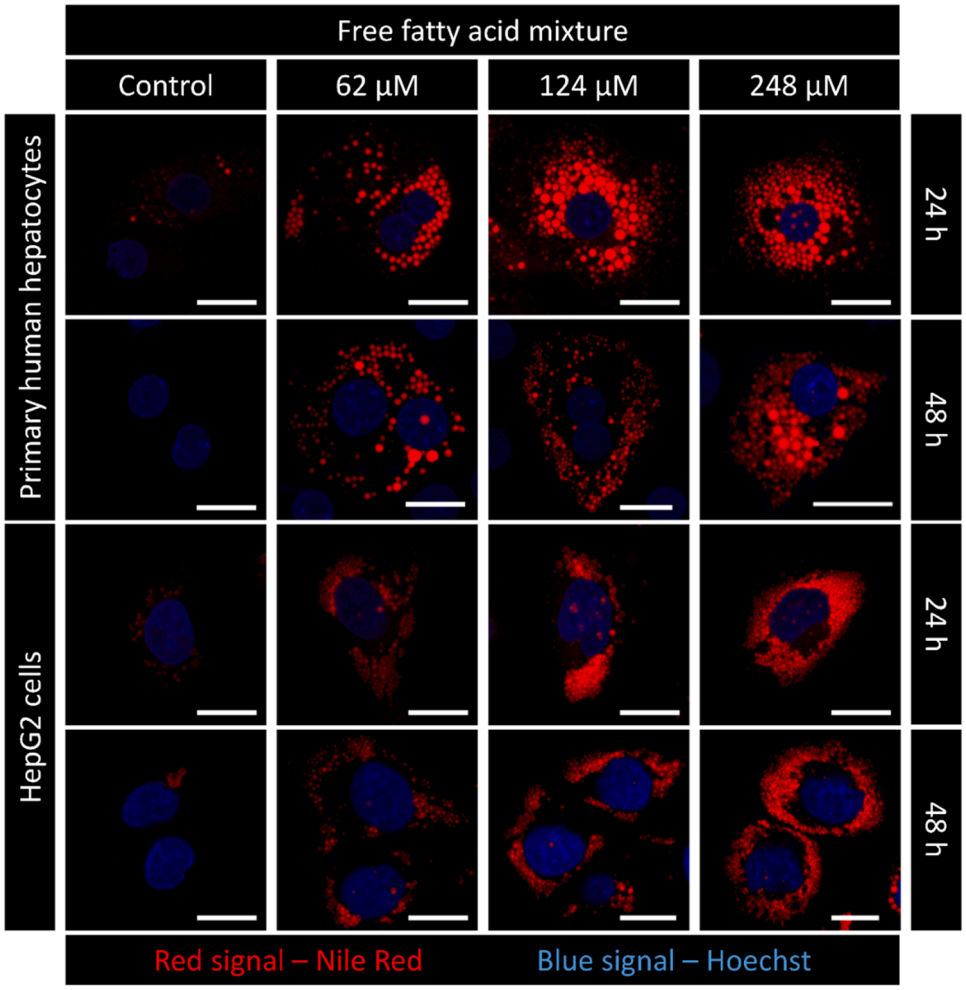

Fig. 1. Visualization of lipid droplets in cultured primary human hepatocytes (PHH) and HepG2 cells by Nile Red. The cells were incubated with oleic acid and palmitic acid in a ratio of 2:1, (free fatty acid mixture) for 24 h and 48 h. Scale bars = 20 µm.

on the Nile Red signal (Fig. 3C), Hoechst signal (Fig. 3D), CTB signal (Fig. 3E) or TMRE signal (Fig. 3F).

Based on the above findings and results of previous reports, we selected an exposure time of 48 h (Albrecht et al., 2019; Gu et al., 2018) for the test compounds, together with 62 µM fatty acid mix (Donato et al., 2012) for subsequent experiments (Fig. 4A).

After co-exposure with the test compound and the fatty acid mix, Nile Red fluorescence was measured to quantify the formation of intracellular lipids. In addition, the signal of the DNA dye Hoechst was quantified for normalization purpose. Using these conditions, we incubated cells with increasing concentrations of two compounds (amiodarone and methotrexate) that are known to induce steatosis (Table 1), and compared the results to two compounds that have not been reported to influence lipid metabolism in hepatocytes (theophylline and zaleplon). In addition to lipid accumulation measurement, cytotoxicity was determined using the CTB assay in PHHs as introduced in a previous study (Albrecht et al., 2019) (Fig. 4B). The results demonstrate that amiodarone and methotrexate caused an increase in lipid formation at non-cytotoxic concentrations as measured with the Nile Red assay, while theophylline and zaleplon treatment had no influence on the Nile Red signal up to cytotoxic concentrations (Fig. 4C), suggesting that lipid accumulation is indeed detectable at lower concentrations than cytotoxicity and therefore may represent a suitable readout for DILI prediction.

To finally investigate if the addition of the fatty acid mix improves the sensitivity of the induction of lipid droplets by steatogenic compounds, we performed the Nile Red assay with and without the addition of the fatty acid mix (FFA) using amiodarone (AMIO), methotrexate (MTX), and valproic acid (VPA) as test compounds. The results show that AMIO and VPA induced an increase in the Nile Red signal even without the addition of the FFA whereas no increase was observed for MTX (Fig. 4D). Upon the addition of FFA, the compound-induced increase in the Nile Red signal was significantly stronger (Fig. 4E), but the extent of the difference due to FFA was relatively small. Considering that previous studies already recommended the use of FFA for in vitro steatosis testing (Donato et al., 2012; Levy et al., 2015; Müller and Sturla, 2019) and that the present results show a moderate improvement, we decided to add the fatty acid mix to the culture medium for all subsequent experiments, despite the relatively small effect size due to FFA.

3.3. *The Nile Red assay improves differentiation of hepatotoxic and non-hepatotoxic compounds*

The results of the two steatogenic and non-steatogenic compounds described in the previous section encouraged us to investigate 60 test compounds for which information is available on whether therapeutic doses cause an increased risk of hepatotoxicity in patients or not. This information is summarized as 'hepatotoxicity reported' (yes/no) (Table 1), while sources and information on type and proposed mechanism of DILI are provided in Supplement 1. Moreover, information is also given on whether the test compound is known to induce steatosis in

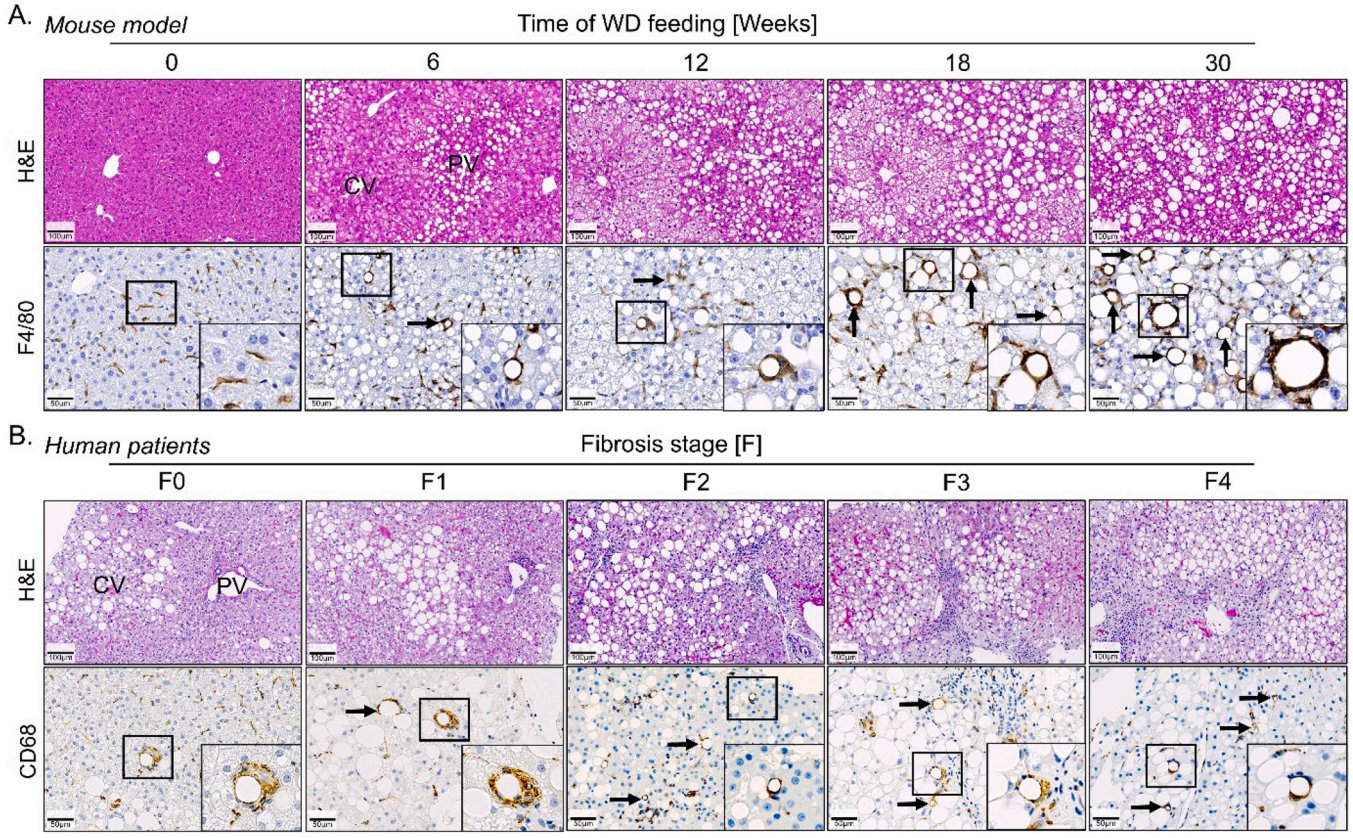

Fig. 2. Lipid droplets in livers of patients with NAFLD (A) and mice fed a Western diet (WD) (B). Upper panel A and B: Hematoxylin & Eosin-stained liver tissue sections; lower panel A and B: Liver tissue sections immunostained with CD68 and F4/80 to visualize macrophage crowns around lipid droplets. Patients of different fibrosis stages were analyzed (F0-F4). The feeding periods with WD ranged from 6 to 30 weeks. Arrows indicate macrophages, CV = central vein, PV = portal vein.

patients (Table 1, Supplement 1) in order to separate the hepatotoxic compounds into substances that may or may not induce steatosis. In the next step, we established and validated pharmacokinetic models for all compounds (Supplement 5), and then simulated the maximal blood concentration (C_{max}), total concentration (i.e., protein bound and free compound) of the upper 95% percentile of 100 virtual subjects from a North European population (Table 1). For all compounds, cells were treated with varying concentrations and the Nile Red assay and the CTB cytotoxicity assay were performed. After modeling of the concentration response curves, the EC_{10} values of both assays were calculated (Table 1).

Next, we studied the ratio of the EC_{10} values for both the CTB and the Nile Red assays (Fig. 5). A ratio (expressed as $\log_2$ change) higher than zero indicated that an increase in lipid droplets was detected at lower concentrations than those causing cytotoxicity. This ratio increased to values higher than 2^5 for the five most extreme substances, indicating that lipid droplets may be induced at concentrations that are much lower than cytotoxic ones.

For 37 substances, a lower concentration was determined for lipid droplet accumulation than for cytotoxicity. One compound, primidone, did not show a positive result in either assay up to the highest concentration tested, and for 22 compounds the CTB assay produced a lower EC_{10} median value than the Nile Red assay. For nine of the 13 in vivo steatosis-inducing substances, lipid droplet accumulation was measured at lower concentrations than cytotoxicity. For seven of these nine compounds, the concentration leading to lipid droplet formation was at least fourfold lower than those inducing cytotoxicity. For the remaining four steatosis-inducing substances, no lipid droplet accumulation could be observed at non-cytotoxic concentrations in the Nile Red assay.

Finally, we studied if the Nile Red assay improves the differentiation of hepatotoxic from non-hepatotoxic compounds when considered in addition to the CTB cytotoxicity test. For this purpose, we calculated the TSI for the EC_{10} of the CTB cytotoxicity test alone, the EC_{10} of the Nile Red assay alone, and the lower EC_{10} of both assays ('combination'). Considering all tested compounds (n = 60), the TSI of the CTB assay, the Nile Red and the combined assays were 0.74, 0.78 and 0.80, respectively (Table 2).

Next, different compound subsets were compared: first, all non-hepatotoxic substances were compared to the hepatotoxic substances that do not induce steatosis (Subset 1); and second, all non-hepatotoxic substances were compared to the hepatotoxic substances that induce steatosis (Subset 2). For the hepatotoxic compounds with reported steatosis (n = 13), the combination of both assays improved the TSI with values of 0.78 (CTB alone), 0.82 (Nile Red alone) and 0.89 (combined assays). In contrast, the combination of both assays led to an only minor increase in the TSI for the hepatotoxic compounds without reported steatosis (n = 18) (Table 2). Thus, the data demonstrate that the Nile Red assay improves the separation of hepatotoxic and non-hepatotoxic compounds compared to a cytotoxicity test alone, particularly for compounds that induce steatosis in patients.

Comparable to the TSI, the TEI was also improved upon using the Nile Red assay resulting in values of 0.71 (CTB alone), 0.78 (Nile Red alone) and 0.88 (combination) for the hepatotoxic compounds with reported steatosis (excluding the hepatotoxic compounds not reported to induce steatosis). To illustrate the in vitro-in vivo relationship between the tested compounds, we plotted the EC_{10} of the respective in vitro tests against the modelled maximal blood concentration resulting from the doses for which hepatotoxicity information (hepatotoxic, non-hepatotoxic in patients) is available. The plots illustrate that the combination of both assays results in improved TSI and TEI compared to the cytotoxicity test alone (Fig. 6). However, six hepatotoxic compounds (rosuvastatin, lovastatin, simvastatin, atorvastatin, clofibrate and

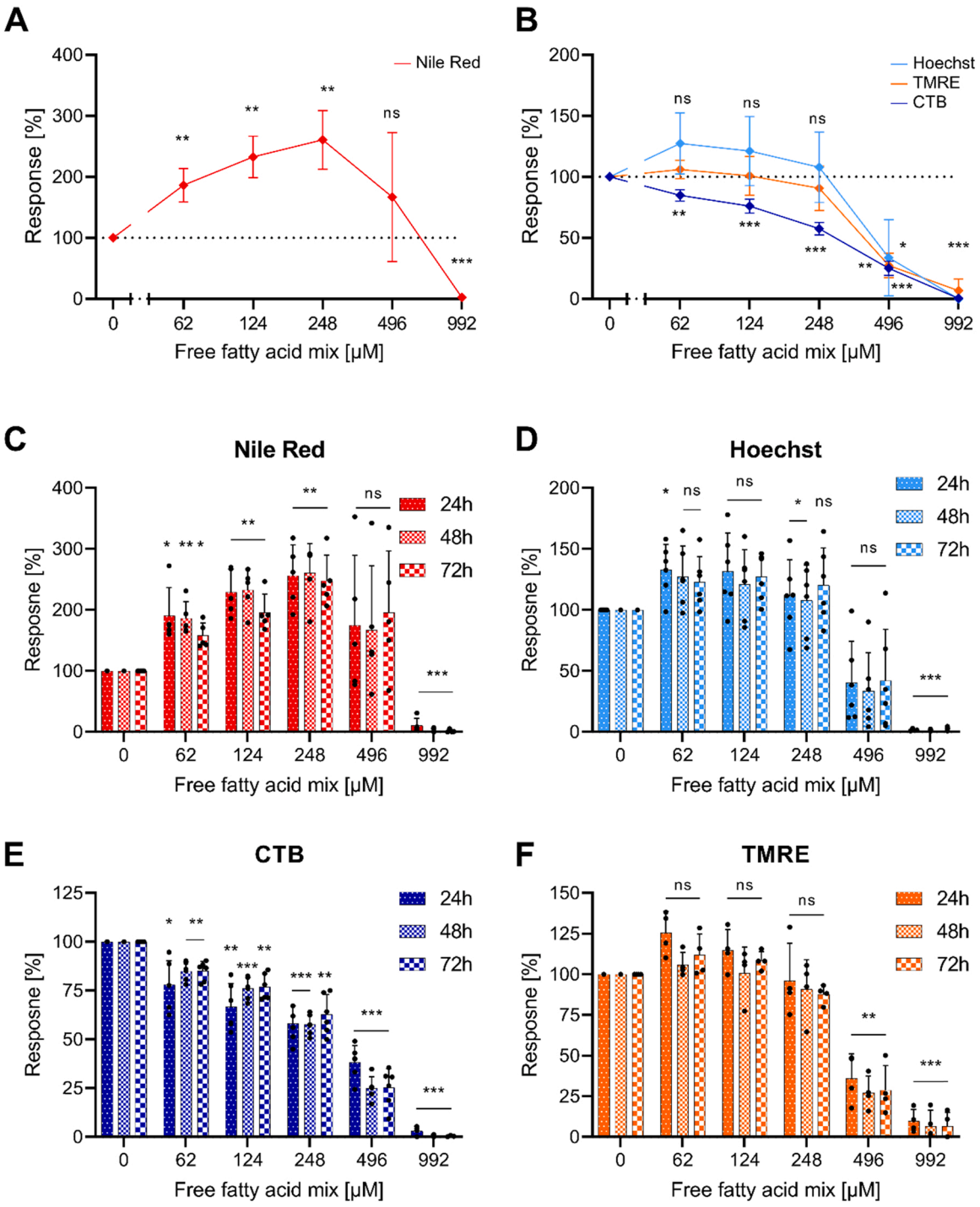

Fig. 3. Optimization of conditions for the Nile Red assay. (A) Concentration-dependent analysis of HepG2 cells incubated with a fatty acid mix (oleic acid and palmitic acid ratio 2:1). (B) Nuclear signal (Hoechst), mitochondrial potential (TMRE) and the CTB cytotoxicity test of the same samples shown in (A). (C-F) Nile Red assay, nuclear (Hoechst) signal, CTB assay and mitochondrial activity (TMRE) of HepG2 cells incubated with increasing concentrations of fatty acid mix for 24, 48 and 72 h. Data are mean values and standard deviations of at least three biological replicates. * indicates $p < 0.05$, * * indicates $p < 0.01$, * ** indicates $p < 0.001$ compared to the respective control (0 µM), Dunnett's multiple comparisons test, ns = non-significant.

stavudine) still remain underestimated, a limitation that will be addressed in the discussion.

4. Discussion

The accumulation of lipid droplets in hepatocytes is a key feature of DILI induced by a subset of hepatotoxic compounds (Begriche et al., 2011; Jaeschke et al., 2002). In the present study, we evaluated an in vitro technique based on the fluorescent dye Nile Red (also called AdipoRed) for the quantification of lipid droplets to learn if this approach generates relevant information with respect to the in vivo situation considering oral doses and blood concentrations of patients. In lipophilic environments, Nile Red shows a strong fluorescence, while it is quenched in aqueous environments (Greenspan et al., 1985). We observed that compounds, such as methotrexate, amiodarone and nifedipine that are known to cause steatosis in patients, induce a strong

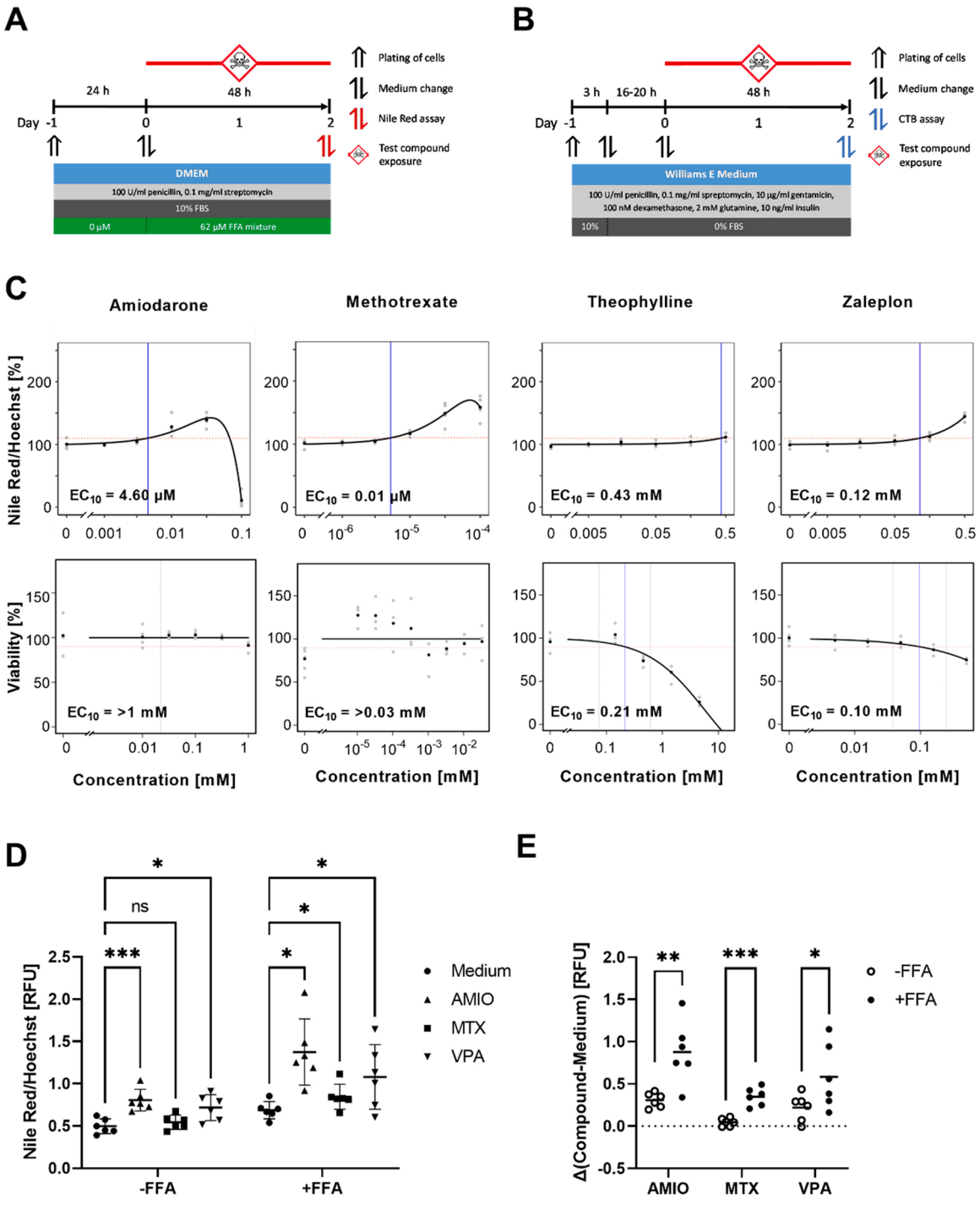

Fig. 4. Nile Red assay for two compounds reported to induce steatosis in humans (amiodarone, methotrexate) and two negative controls (theophylline, zaleplon). (A) Experimental schedule for the Nile Red assay (HepG2). (B) Experimental schedule for the CTB cytotoxicity assay (PHH). (C) Examples of concentration response curves derived from the Nile Red (top panel) and CTB (bottom panel) assay. Grey dots represent the results of at least three technical replicates, black dots denote the concentration-wise mean. The vertical blue lines indicate the EC_{10} and the dotted grey line the confidence interval. Data of all compounds (n = 60) are given in Supplement 3. (D) and (E) Influence of co-incubation with 62 µM fatty acid mixture on 31.6 µM amiodarone (AMIO)-, 0.0316 µM methotrexate (MTX)-, and 1250 µM valproic acid (VPA)-induced lipid accumulation. Data are represented as mean ± SD for 6 biological replicates; * indicates $p < 0.05$, * * indicates $p < 0.01$, * ** indicates $p < 0.001$, Holm-Sidak's multiple comparisons test (D), paired t test (E), ns = non-significant.

increase in lipid droplets in the Nile Red assay. Importantly, lipid droplet accumulation was observed at sub-cytotoxic concentrations for several steatosis-inducing compounds. For example, the median EC_{10} of methotrexate in the Nile Red assay was 0.0056 µM; whereas, no cytotoxicity was observed in the CTB assay up to concentrations of 33 µM. Similarly, amiodarone induced an accumulation of lipid droplets with an EC_{10} of 5 µM but was not cytotoxic up to 1000 µM. These results encouraged us to analyze a set of 60 compounds and to study how well hepatotoxic and non-hepatotoxic compounds can be differentiated (i) by the CTB cytotoxicity test alone (using the EC_{10} value), and (ii) by a combination of the cytotoxicity and Nile Red assay (using the median EC_{10} of the more sensitive of the two assays).

To assess how well hepatotoxic and non-hepatotoxic compounds were separated, the recently established Toxicity Separation Index (TSI)

Table 1
Overview of all analyzed compounds. The hepatotoxicity status indicates if an increased risk of DILI has been reported for the therapeutic doses in Supplement 5. Similarly, the steatosis status indicates if therapeutic doses of the respective compounds were reported to cause steatosis in patients Supplement 1. The maximal blood concentration, C_{max} (total concentration, 95% percentile), was obtained by PBPK modeling of therapeutic doses as described in Supplement 5. The in vitro cytotoxicity was obtained by the CTB assay; median and ranges of at least three biological replicates are given. Lipid droplets were quantified by the Nile Red assay. Median and ranges of three biological replicates are given. All raw and processed data are given in Supplement 2.

Compound	Abbreviation	Hepatotoxicity reported	Steatosis reported in vivo	In vivo Cmax whole blood 95% total [mM]	In vitro cytotoxicity EC_{10} [mM] median[min/max]	In vitro lipid accumulation EC_{10} [mM] median[min/max]
Acetaminophen	APAP	no	no	1.09×10^{-01}	1.403 [0.5/2.833]	0.561 [0.259/0.997]
Acetaminophen	APAP	yes	no	$1.21 \times 10^{+00}$	1.403 [0.5/2.833]	0.561 [0.259/0.997]
Amiodarone	AMIO	yes	yes	3.70×10^{-04}	> 1 [> 1/> 1]	0.005 [0.004/0.008]
Aspirin	ASP	yes	yes	2.40×10^{-01}	4.115 [0.335/> 10]	2.132 [1.044/4.774]
Atorvastatin	AVS	yes	no	1.50×10^{-05}	0.138 [0.065/0.208]	0.045 [0.029/> 0.1]
Atropine	ATRO	no	no	5.38×10^{-06}	2.238 [0.074/> 3.16]	0.111 [0.107/0.188]
Benzbromarone	BZB	yes	no	1.79×10^{-02}	0.01 [0.010/0.012]	0.037 [0.037/0.038]
Benztropine	BZT	no	no	1.23×10^{-05}	0.011 [0.007/0.038]	0.002 [0.002/0.002]
Bosentan	BOS	yes	no	2.81×10^{-03}	0.0175 [0.0033/0.0554]	0.0272 [0.0149/0.0278]
Buspirone	BPR	no	no	2.90×10^{-05}	0.0129 [0.0089/0.0258]	0.016 [0.0153/0.0199]
Carbamazepine	CBZ	yes	yes	1.81×10^{-02}	0.009 [0.002/0.020]	0.076 [0.064/0.090]
Chlorpheniramine	CHL	no	no	6.49×10^{-05}	0.044 [0.014/0.155]	0.007 [0.007/0.013]
Clofibrate	CLFI	yes	no	1.47×10^{-05}	> 1 [> 1/> 1]	0.167 [0.166/> 1]
Clonidine	CLON	no	no	9.40×10^{-06}	0.317 [0.057/0.555]	0.124 [0.119/0.229]
Codeine	COD	no	no	2.33×10^{-04}	0.956 [0.536/1.058]	0.082 [0.052/0.223]
Cyclosporin A	CSA	yes	yes	7.34×10^{-03}	0.014 [0.008/0.031]	0.003 [0.002/0.007]
Diclofenac	DFN	yes	no	5.42×10^{-03}	0.115 [0.036/0.143]	0.076 [0.067/0.115]
Digoxin	DIGI	no	no	2.15×10^{-06}	0.000066 [0.000046/0.000136]	0.000083 [0.000026/> 0.000316]
Diphenhydramine	DPH	no	no	5.90×10^{-04}	0.122 [0.056/0.143]	0.008 [0.007/0.012]
Dimethyl sulfoxide	DMSO	no	no	1.08×10^{-01}	> 1400 [21.47/> 1400]	379.19 [124.13/747.93]
Entacapone	ETC	yes	no	9.94×10^{-03}	0.02 [0.017/0.034]	0.037 [0.031/0.038]
Ethanol	ETOH	no	no	5.76×10^{-03}	10.22 [2.05/170.50]	274.7 [65.90/> 1000]
Ethanol	ETOH	yes	yes	$1.01 \times 10^{+01}$	10.22 [2.05/170.50]	274.7 [65.90/> 1000]
Glucose	GLC	no	no	$7.15 \times 10^{+00}$	119.71 [71.94/> 316]	19.45 [16.36/79.22]
Hydroxyzine	HYZ	no	no	4.94×10^{-04}	0.079 [0.045/0.094]	> 0.5 [> 0.5/> 0.5]
Ibuprofen	IBU	yes	yes	2.53×10^{-01}	1.992 [0.948/2.056]	0.411 [0.226/0.426]
Indomethacin	INDO	yes	no	3.48×10^{-03}	> 0.245 [0.081/> 0.245]	0.077 [0.038/> 0.1]
Isosorbide dinitrate	ISS	no	no	1.03×10^{-04}	0.108 [0.098/0.135]	0.192 [0.083/0.262]
Ketoconazole	KC	yes	no	1.62×10^{-02}	0.026 [0.008/0.100]	0.002 [0.002/0.019]
Lovastatin	LO	yes	no	8.48×10^{-06}	> 0.245 [0.024/> 0.245]	0.034 [0.018/> 0.316]
Melatonin	MEL	no	no	2.70×10^{-05}	0.687 [0.040/> 5]	0.801 [0.327/1.021]
Methotrexate	MTX	yes	yes	1.03×10^{-03}	> 0.033 [> 0.033/> 0.033]	5.6E-06 [0.0000053/0.0000058]
N-Acetylcysteine	NAC	no	no	3.19×10^{-03}	> 10 [0.243/> 10]	2.06 [0.388/6.221]
Nifedipine	NDP	yes	yes	1.16×10^{-03}	> 0.432 [> 0.432/> 0.432]	0.012 [0.008/0.012]
Oxycodone	OXC	no	no	9.84×10^{-05}	1.149	0.177

(*continued on next page*)

Table 1 (*continued*)

Compound	Abbreviation	Hepatotoxicity reported	Steatosis reported in vivo	In vivo Cmax whole blood 95% total [mM]	In vitro cytotoxicity EC_{10} [mM] median[min/max]	In vitro lipid accumulation EC_{10} [mM] median[min/max]
					[0.546/6.337]	[0.139/0.221]
Oxymorphone	OXM	no	no	1.13×10^{-05}	0.028	1.021
					[0.024/0.043]	[0.338/1.315]
Pazopanib	PZB	yes	no	6.20×10^{-02}	> 0.189	0.008
					[> 0.189/> 0.189]	[0.007/0.009]
Perhexiline	PRX	yes	yes	8.69×10^{-04}	0.004	> 0.05
					[0.003/0.006]	[> 0.05/> 0.05]
Pindolol	PIN	no	no	1.71×10^{-04}	> 0.5	0.062
					[> 0.5/> 0.5]	[0.049/0.129]
Pioglitazone	PIO	yes	no	5.33×10^{-03}	0.009	0.036
					[0.008/0.08]	[0.002/0.047]
Primaquine	PRIMA	no	no	6.63×10^{-04}	0.001	0.022
					[0.001/0.027]	[0.009/0.026]
Primidone	PRI	no	no	5.48×10^{-02}	> 0.5	> 0.5
					[> 0.5/> 0.5]	[0.0859/> 0.5]
Promethazine	PMZ	no	no	3.27×10^{-05}	0.014	0.002
					[0.004/0.032]	[0.002/0.002]
Propranolol	PPL	no	no	2.35×10^{-04}	0.021	> 0.316
					[0.003/0.080]	[0.006/> 0.316]
Pyridoxine	PDX	no	no	7.04×10^{-05}	1.023	> 3.16
					[0.1055/5.082]	[> 3.16/> 3.16]
Rifampicin	RIF	yes	no	2.01×10^{-02}	0.262	0.033
					[0.121/0.424]	[0.020/0.046]
Rosiglitazone	RGZ	yes	no	5.99×10^{-04}	0.036	0.003
					[0.034/0.047]	[0.003/0.092]
Rosuvastatin	ROS	yes	no	9.78×10^{-06}	0.028	0.001
					[0.026/0.028]	[0.00/0.002]
Simvastatin	SIM	yes	no	2.15×10^{-05}	0.02	> 0.5
					[0.013/0.046]	[> 0.5/> 0.5]
Sitaxentan	SXS	yes	no	1.73×10^{-02}	0.132	0.054
					[0.086/0.184]	[0.034/0.077]
4-Phenylbutyrate	SPB	no	no	9.11×10^{-01}	1.969	1.044
					[0.192/> 10]	[0.757/1.442]
Stavudine	STAVU	yes	yes	2.41×10^{-03}	0.92	0.869
					[0.913/1.911]	[0.830/> 10]
Tetracycline	TC	yes	yes	1.55×10^{-02}	0.397	0.088
					[0.397/> 1]	[0.060/0.102]
Theophylline	THE	no	no	6.10×10^{-02}	0.214	0.43
					[0.205/0.945]	[0.204/> 0.5]
Tolcapone	TOLC	yes	no	1.06×10^{-02}	0.028	0.029
					[0.02/0.031]	[0.008/0.039]
Tolterodine	TTD	no	no	1.55×10^{-05}	0.035	0.004
					[0.025/0.128]	[0.003/0.008]
Triclosan	TSN	no	no	2.60×10^{-04}	0.136	> 0.0316
					[0.047/0.250]	[0.007/> 0.0316]
Triprolidine	TPL	no	no	3.16×10^{-05}	0.161	0.011
					[0.122/> 1.6]	[0.010/0.013]
Troglitazone	TROG	yes	yes	2.21×10^{-03}	0.011	> 1
					[0.010/0.022]	[> 1/> 1]
Valproic acid	VPA	yes	yes	5.69×10^{-01}	10.13	0.765
					[8.46/22.13]	[0.393/2.259]
Vitamin C	VITC	no	no	6.98×10^{-03}	3.701	2.877
					[0.283/> 31.6]	[0.731/> 3.16]
Zaleplon	ZAL	no	no	1.94×10^{-04}	0.097	0.115
					[0.016/> 0.5]	[0.077/0.366]

was applied (Albrecht et al., 2019; Sachinidis et al., 2019). The results showed that the combination of both assays improved the TSI compared to using the CTB cytotoxicity test alone. This was particularly evident when hepatotoxic compounds that are also known to induce steatosis in patients were compared to non-hepatotoxic compounds. For this set of compounds, the TSI was improved from 0.78 for the CTB cytotoxicity test only to 0.89 for the combination of both assays. The size of this effect is relevant if one considers that a TSI of 1.0 means a perfect separation of hepatotoxic and non-hepatotoxic compounds, while a random result would lead to a TSI of 0.5 (Sachinidis et al., 2019). The combination of both assays also improved the Toxicity Estimation Index (TEI) from 0.71 (CTB test alone) to 0.88 for the combination. An improved TEI is relevant if one aims to estimate a C_{max} in human blood based on the in vitro data of a test compound (Albrecht et al., 2019).

In the present study, we investigated a set of relatively well-characterized 'gold standard compounds' (Sachinidis et al., 2019). Under these conditions, the here introduced Nile Red assay allowed a relatively good differentiation of hepatotoxic compounds known to induce steatosis from non-hepatotoxic compounds. However, it should be considered that the analyzed gold standard compounds cannot be considered to be representative of all hepatotoxic compounds. Therefore, a next step would be the analysis of a larger (n > 200) number of representative hepatotoxic and non-hepatotoxic compounds, and the readouts should include in vitro assays measuring further mechanisms relevant for DILI. Moreover, it still has to be analyzed if in vitro readouts will improve DILI prediction compared to already existing methods, such as the Biopharmaceutics Drug Disposition Classification System (BDDCS), where highly permeable and extensively metabolized compounds have been shown to have a higher DILI risk (Chan and Benet, 2018, 2017; Wu and Benet, 2005).

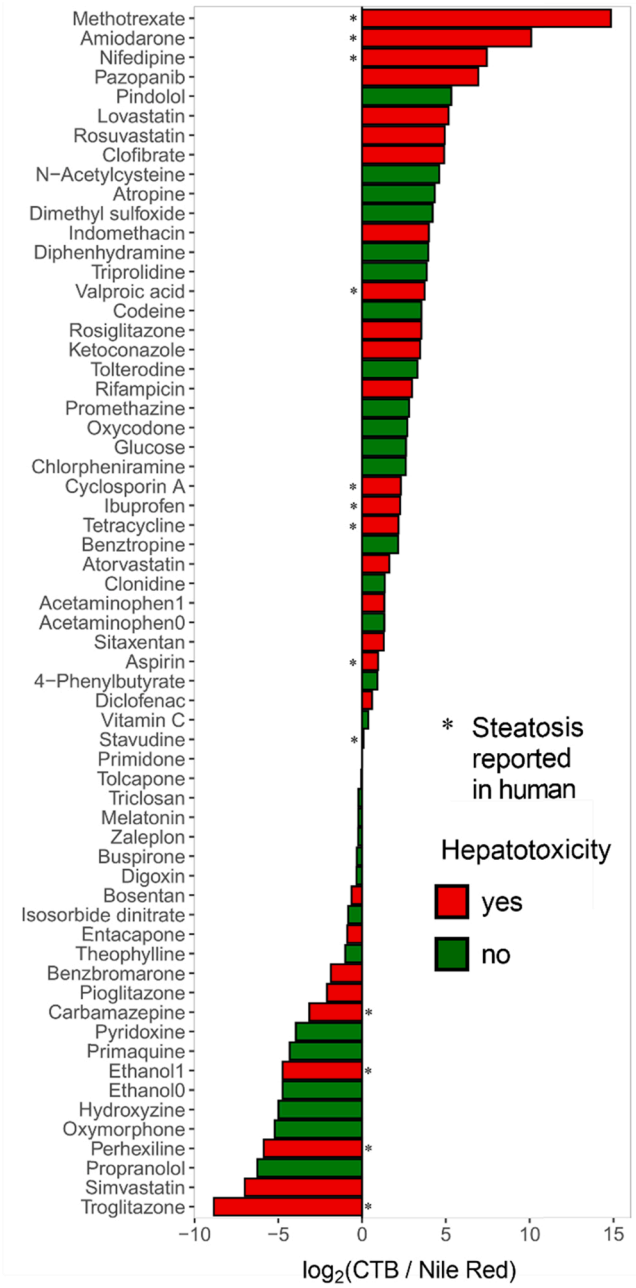

Fig. 5. Ratio of the EC_{10} values of the CTB cytotoxicity test (PHH) and the Nile Red assay (HepG2) for all 60 analyzed compounds. Ratios were calculated by dividing the EC_{10} (median) values measured with the CTB assay by those obtained with the Nile Red assay and log_2 values of the respective ratios are shown. The hepatotoxicity status is indicated by the red and green color of the bars. * indicates steatosis-inducing compounds. Compounds were considered as steatosis-inducing based on previous publications. A detailed list with the respective references is given in Supplement 1.

It should be considered that some compounds that cause steatosis in vivo, such as troglitazone and perhexiline, did not induce lipid droplet accumulation in the present in vitro study. Other compounds, such as carbamazepine and ethanol increased lipid droplets only at cytotoxic concentrations. This discrepancy to the in vivo situation may be explained by the lack of metabolic activation particularly by Cyp450 enzymes in HepG2 cells (Westerink and Schoonen, 2007). One example is troglitazone, which is known to be metabolized to a reactive metabolite and for which no increased lipid accumulation was detected up to the highest tested concentration.It was shown that troglitazone and its main metabolite troglitazone sulfate inhibit BSEP and MRP4 which play a role in the bile acid efflux (Daly, 2017). The inhibition leads to increased intracellular bile acid concentrations which can result in cytotoxicity. Furthermore, a reactive metabolite of troglitazone induces cytotoxicity by mitochondrial impairment and GSH depletion (Dragovic et al., 2016). However, the role of troglitazone and its reactive metabolite for hepatotoxicity is still discussed controversially (Masubuchi, 2006). By using two cell systems, HepG2 and PHH, and using the result of the more susceptible cells, it is still possible to detect the before mentioned substances at in vivo relevant concentrations. Although these substances are classified as steatotic based on published studies, this might not be the main or the only mechanism of how hepatotoxicity is induced. For example in case of perhexiline endoplasmic reticulum stress plays a major role in cytotoxicity (Ren et al., 2021) but also an accumulation of protonated perhexiline which leads to mitochondrial impairment and consequently inhibition of fatty acid metabolism (Dragovic et al., 2016). This supports the use of an in vitro test battery with a variety of assays covering DILI relevant mechanisms and the inclusion of different cell systems, which have different advantages and disadvantages.

Table 2
Toxicity Separation Index (TSI) and Toxicity Estimation Index (TEI) for the CTB and Nile Red assay alone and in combination. Values are based on EC_{10} median values for all compounds and different subsets. Subset 1 includes all non-hepatotoxic compounds (n = 31) and all hepatotoxic compounds that do not induce steatosis in vivo (n = 18). Subset 2 includes all non-hepatotoxic compounds (n = 31) and all hepatotoxic once that are reported to induce steatosis in vivo (n = 13). All TSI and TEI values can be found in Supplement 2.

		All compounds non-hepatotoxic (n = 31) vs. hepatotoxic (n = 31)		Subset 1 non-hepatotoxic (n = 31) vs. hepatotoxic, non-steatosis inducing (n = 18)		Subset 2 non-hepatotoxic (n = 31) vs. hepatotoxic, steatosis inducing (n = 13)	
Assay	**EC cutoff**	**TSI**	**TEI**	**TSI**	**TEI**	**TSI**	**TEI**
CTB	EC_{10} median	0.74	0.67	0.71	0.65	0.78	0.71
Nile Red	EC_{10} median	0.78	0.74	0.76	0.72	0.82	0.78
Combination	EC_{10} median	0.80	0.81	0.75	0.70	0.89	0.88

A limitation of the present study with the combined CTB and Nile Red assays is that six hepatotoxic compounds, indicated in Fig. 6C, still cluster within the non-hepatotoxic substances, thereby underestimating their DILI risk. It is notable that four of the six underestimated substances belong to the group of statins, suggesting a class-specific effect. The hepatotoxicity of statins is relatively rare but has been well documented with varying prevalence for the different drugs (Björnsson, 2017). A possible explanation why these four substances are not detected at physiologically-relevant concentrations may be that a different mechanism is responsible for their hepatotoxicity. In addition, it cannot be excluded that these substances cause damage by several different mechanisms, and the analysis of cytotoxicity and lipid droplet formation performed here with the CTB and Nile red assays, respectively, is not sufficient. The fact that hepatotoxic events of statins are so rare may speak for an idiosyncratic effect, which cannot be detected with this test system but the mechanism remains unknown (Mach et al., 2018). Interestingly, the DILI risk of the lipid lowering agent clofibrate has previously also been underestimated. A study from Qu et al. (2001) performed in isolated mouse liver mitochondria and a hepatocyte cell line suggests impaired mitochondrial function and increased ROS production as a possible mechanism. Furthermore, it was shown that clofibrate increases CYP4A11 expression in primary human hepatocytes. Thus, interference with hepatic enzyme function may represent another possible mechanism for clofibrates hepatotoxicity (Raucy et al., 2004). The mechanism of stavudine associated hepatotoxicity is not clearly defined but in vitro studies revealed mitochondrial dysfunction and

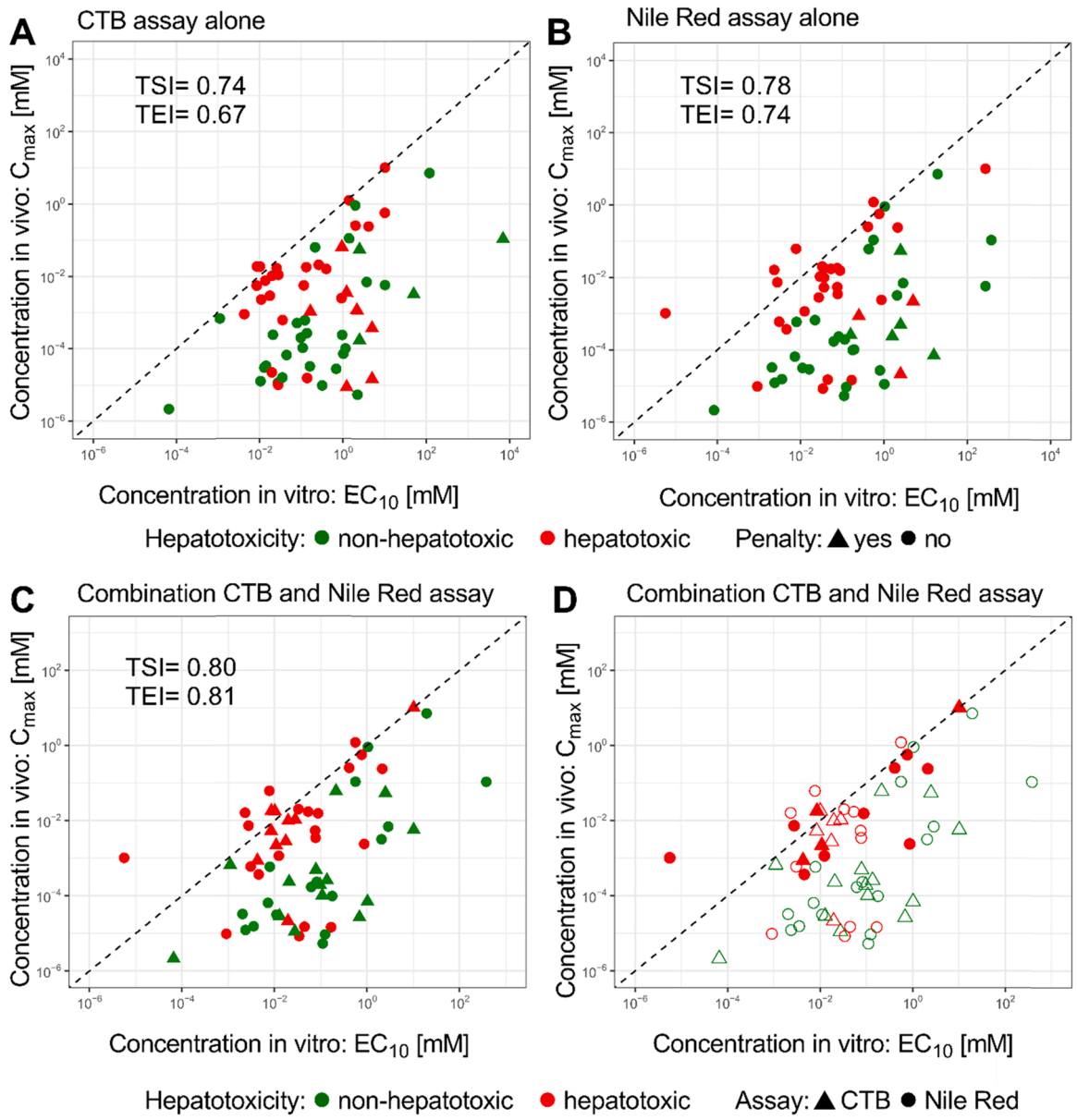

Fig. 6. In vitro-in vivo extrapolation plots using the EC_{10} median values (x-axis) and the C_{max} (total concentration in blood; 95%-CI) (y-axis) for the CTB cytotoxicity test alone (A) and the Nile Red assay alone (B). Compounds which did not result in EC_{10} values up to the highest tested concentration are indicated by triangles (penalty: see methods). (C) and (D) The combined analysis, where the more sensitive of the two assays was applied based on the lower value of either the CTB test (triangle) or the Nile Red assay (circle). In (D), the reported steatosis inducing substances are indicated with filled symbols. The dotted lines in A-D are iso-concentration lines that indicate identical concentrations for the x- and y-axes. The red and green symbols represent known hepatotoxic and non-hepatotoxic compounds in patients. APAP and EtOH are included by two symbols, since both hepatotoxic (red) and non-hepatotoxic (green) doses and blood concentrations are known (see Table 1).

increased ROS production (Pillaye et al., 2020; Velsor et al., 2004).

A further limitation of the present study is that the analysis of 60 compounds in the Nile Red assay was performed in HepG2 cells and not yet in primary human hepatocytes. The reason for this choice is that we observed comparable accumulation of fatty acid-induced lipid droplets in both the HepG2 cells and the cultivated human hepatocytes. Similarly, previous studies reported that HepG2 cells maintained the capacity to form lipid droplets in response to steatosis-inducing drugs (Donato et al., 2012; Levy et al., 2015; Müller and Sturla, 2019). Therefore, we decided to perform the Nile Red assay with HepG2 cells in order to learn if this readout improves the differentiation of hepatotoxic and non-hepatotoxic compounds. Since this was confirmed in the present study, a subsequent step would be to determine if the Nile Red assay performed in primary human hepatocytes would lead to even better results than HepG2 cells. It should however be considered that such a study would require tremendous effort and costs, since hepatocytes from several donors would have to be analyzed to consider possible inter-individual differences. In contrast, the CTB cytotoxicity tests were already performed with PHHs, since this assay was already optimized in a 96-well format with cryopreserved hepatocytes (Albrecht et al., 2019). For both the CTB cytotoxicity and the Nile Red assay it remains to be analyzed if more elaborate 3D systems (Bell et al., 2018; Serras et al., 2021; Weaver et al., 2020) would yield an even higher TSI and TEI.

In conclusion, we established an in vitro assay that detects the accumulation of lipid droplets and in combination with a cytotoxicity test improves the differentiation of the here-studied hepatotoxic and non-hepatotoxic compounds compared to the analysis of cytotoxicity alone.

Funding statement

This work received funding from the European Union's Horizon 2020 research and innovation program under grant agreement no. 681002 (EU-ToxRisk) and LivSysTransfer (BMBF, 031L0119) and the BMBF projects SteatoTox (161L0114B) and SysBioTop-Moving (161L0243C). This work has been supported (in part) by the Research Training Group "Biostatistical Methods for High-Dimensional Data in Toxicology" (RTG 2624, Project P1 and P2) funded by the Deutsche Forschungsgemeinschaft (DFG, German Research Foundation - Project Number 427806116). AG is funded by the German Research Foundation (DFG; GH 276/1-1; Project Number 457840828). Özlem Demirci Turgunbayer was supported by the 2219-TUBITAK International Post Doctoral Research Fellowship Program. This work was financially supported by the DFG Grant ZE1037/1-3, the BMBF Grants SteatoTox 031L0114A and SteatoTox-2 16LW0116k to A.Z.

Declaration of Competing Interest

The authors declare that they have no known competing financial interests or personal relationships that could have appeared to influence the work reported in this paper.

Data availability

All data are available on request or in the supplementary material.

Acknowledgments

We would like to thank Certera UK (Simcyp Division) for granting free access to the Simcyp Simulators through an academic license (subject to conditions).

Appendix A. Supporting information

Supplementary data associated with this article can be found in the online version at doi:10.1016/j.toxlet.2022.08.006.

References

Akaike, H., 2011. Akaike's Information Criterion, in: International Encyclopedia of Statistical Science. Springer Berlin Heidelberg, pp. 25–25. https://doi.org/10.1007/978–3-642–04898-2_110.

Albrecht, W., Kappenberg, F., Brecklinghaus, T., Stoeber, R., Marchan, R., Zhang, M., Ebbert, K., Kirschner, H., Grinberg, M., Leist, M., Moritz, W., Cadenas, C., Ghallab, A., Reinders, J., Vartak, N., van Thriel, C., Golka, K., Tolosa, L., Castell, J.V., Damm, G., Seehofer, D., Lampen, A., Braeuning, A., Buhrke, T., Behr, A.C., Oberemm, A., Gu, X., Kittana, N., van de Water, B., Kreiling, R., Fayyaz, S., van Aerts, L., Smedsrød, B., Ellinger-Ziegelbauer, H., Steger-Hartmann, T., Gundert-Remy, U., Zeigerer, A., Ullrich, A., Runge, D., Lee, S.M.L., Schiergens, T.S., Kuepfer, L., Aguayo-Orozco, A., Sachinidis, A., Edlund, K., Gardner, I., Rahnenführer, J., Hengstler, J.G., 2019. Prediction of human drug-induced liver injury (DILI) in relation to oral doses and blood concentrations. Arch. Toxicol. 93, 1609–1637. https://doi.org/10.1007/s00204-019-02492-9.

Barbero-Becerra, V.J., Giraudi, P.J., Chávez-Tapia, N.C., Uribe, M., Tiribelli, C., Rosso, N., 2015. The interplay between hepatic stellate cells and hepatocytes in an in vitro model of NASH. Toxicol. Vitr 29, 1753–1758. https://doi.org/10.1016/j.tiv.2015.07.010.

Begriche, K., Massart, J., Robin, M.A., Borgne-Sanchez, A., Fromenty, B., 2011. Drug-induced toxicity on mitochondria and lipid metabolism: Mechanistic diversity and deleterious consequences for the liver. J. Hepatol. 54, 773–794. https://doi.org/10.1016/j.jhep.2010.11.006.

Bell, C.C., Dankers, A.C.A., Lauschke, V.M., Sison-Young, R., Jenkins, R., Rowe, C., Goldring, C.E., Park, K., Regan, S.L., Walker, T., Schofield, C., Baze, A., Foster, A.J., Williams, D.P., van de Ven, A.W.M., Jacobs, F., van Houdt, J., Lähteenmäki, T., Snoeys, J., Juhila, S., Richert, L., Ingelman-Sundberg, M., 2018. Comparison of hepatic 2D sandwich cultures and 3d spheroids for long-term toxicity applications: a multicenter study. Toxicol. Sci. 162, 655–666. https://doi.org/10.1093/toxsci/kfx289.

Björnsson, E.S., 2017. Hepatotoxicity of statins and other lipid-lowering agents. Liver Int. 37, 173–178. https://doi.org/10.1111/LIV.13308.

Brain, P., Cousens, R., 1989. An equation to describe dose responses where there is stimulation of growth at low doses. Weed Res 29, 93–96. https://doi.org/10.1111/j.1365-3180.1989.tb00845.x.

Brecklinghaus, T., Albrecht, W., Kappenberg, F., Duda, J., Vartak, N., Edlund, K., Marchan, R., Ghallab, A., Cadenas, C., Günther, G., Leist, M., Zhang, M., Gardner, I., Reinders, J., Russel, F.G., Foster, A.J., Williams, D.P., Damle-Vartak, A., Grandits, M., Ecker, G., Kittana, N., Rahnenführer, J., Hengstler, J.G., 2022. The hepatocyte export carrier inhibition assay improves the separation of hepatotoxic from non-hepatotoxic compounds. Chem. Biol. Interact. 351, 109728 https://doi.org/10.1016/j.cbi.2021.109728.

Bretz, F., Pinheiro, J.C., Branson, M., 2005. Combining multiple comparisons and modeling techniques in dose-response studies. Biometrics 61, 738–748. https://doi.org/10.1111/j.1541-0420.2005.00344.x.

Campos, G., Schmidt-Heck, W., De Smedt, J., Widera, A., Ghallab, A., Pütter, L., González, D., Edlund, K., Cadenas, C., Marchan, R., Guthke, R., Verfaillie, C., Hetz, C., Sachinidis, A., Braeuning, A., Schwarz, M., Weiß, T.S., Banhart, B.K., Hoek, J., Vadigepalli, R., Willy, J., Stevens, J.L., Hay, D.C., Hengstler, J.G., Godoy, P., 2020. Inflammation-associated suppression of metabolic gene networks in acute and chronic liver disease. Arch. Toxicol. 94, 205–217. https://doi.org/10.1007/s00204-019-02630-3.

Chan, R., Benet, L.Z., 2018. Measures of BSEP inhibition in vitro are not useful predictors of DILI. Toxicol. Sci. 162, 499–508. https://doi.org/10.1093/toxsci/kfx284.

Chan, R., Benet, L.Z., 2017. Evaluation of DILI predictive hypotheses in early drug development. Chem. Res. Toxicol. 30, 1017–1029. https://doi.org/10.1021/acs.chemrestox.7b00025.

CRAN - Package DoseFinding [WWW Document], 2019. URL https://cran.r-project.org/web/packages/DoseFinding/index.html (accessed 5.10.21).

Cui, W., Chen, S.L., Hu, K.Q., 2010. Quantification and mechanisms of oleic acid-induced steatosis in HepG2 cells. Am. J. Transl. Res. 2, 95–104.

Daly, A.K., 2017. Drug-induced liver disease. Compr. Med. Chem. III 4–8, 204–216. https://doi.org/10.1016/B978-0-12-409547-2.12382-0.

Dawson, S., Stahl, S., Paul, N., Barber, J., Kenna, J.G., 2012. In vitro inhibition of the bile salt export pump correlates with risk of cholestatic drug-induced liver injury in humans. Drug Metab. Dispos. 40, 130–138. https://doi.org/10.1124/DMD.111.040758.

Donato, M.T., Lahoz, A., Jiménez, N., Pérez, G., Serralta, A., Mir, J., Castell, J.V., Gómez-Lechón, M.J., 2006. Potential impact of steatosis on cytochrome P450 enzymes of human hepatocytes isolated from fatty liver grafts. Drug Metab. Dispos. 34, 1556–1562. https://doi.org/10.1124/dmd.106.009670.

Donato, M.T., Tolosa, L., Jiménez, N., Castell, J.V., Gómez-Lechón, M.J., 2012. High-content imaging technology for the evaluation of drug-induced steatosis using a multiparametric cell-based assay. J. Biomol. Screen 17, 394–400. https://doi.org/10.1177/1087057111427586.

Dragovic, S., Vermeulen, N.P.E., Gerets, H.H., Hewitt, P.G., Ingelman-Sundberg, M., Park, B.K., Juhila, S., Snoeys, J., Weaver, R.J., 2016. Evidence-based selection of training compounds for use in the mechanism-based integrated prediction of drug-induced liver injury in man. Arch. Toxicol. 90, 2979. https://doi.org/10.1007/S00204-016-1845-1.

Gerussi, A., Natalini, A., Antonangeli, F., Mancuso, C., Agostinetto, E., Barisani, D., Di Rosa, F., Andrade, R., Invernizzi, P., 2021. Immune-mediated drug-induced liver injury: immunogenetics and experimental models. Int. J. Mol. Sci. 22. https://doi.org/10.3390/IJMS22094557.

Ghallab, A., Hassan, R., Hofmann, U., Friebel, A., Hobloss, Z., Brackhagen, L., Begher-Tibbe, B., Myllys, M., Reinders, J., Overbeck, N., Sezgin, S., Zühlke, S., Seddek, A., Murad, W., Brecklinghaus, T., Kappenberg, F., Rahnenführer, J., González, D., Goldring, C., Copple, I.M., Marchan, R., Longerich, T., Vucur, M., Luedde, T., Urban, S., Canbay, A., Schreiter, T., Trauner, M., Akakpo, J.Y., Olyaee, M., Curry, S.C., Sowa, J.-P., Jaeschke, H., Hoehme, S., Hengstler, J.G., 2022. Interruption of bile acid uptake by hepatocytes after acetaminophen overdose ameliorates hepatotoxicity. J. Hepatol. https://doi.org/10.1016/j.jhep.2022.01.020.

Ghallab, A., Hofmann, U., Sezgin, S., Vartak, N., Hassan, R., Zaza, A., Godoy, P., Schneider, K.M., Guenther, G., Ahmed, Y.A., Abbas, A.A., Keitel, V., Kuepfer, L., Dooley, S., Lammert, F., Trautwein, C., Spiteller, M., Drasdo, D., Hofmann, A.F., Jansen, P.L.M., Hengstler, J.G., Reif, R., 2019. Bile microinfarcts in cholestasis are initiated by rupture of the apical hepatocyte membrane and cause shunting of bile to sinusoidal blood. Hepatology 69, 666–683. https://doi.org/10.1002/hep.30213.

Ghallab, A., Myllys, M., Friebel, A., Duda, J., Edlund, K., Halilbasic, E., Vucur, M., Hobloss, Z., Brackhagen, L., Begher-Tibbe, B., Hassan, R., Burke, M., Genc, E., Frohwein, L.J., Hofmann, U., Holland, C.H., González, D., Keller, M., Seddek, A.L., Abbas, T., Mohammed, E.S.I., Teufel, A., Itzel, T., Metzler, S., Marchan, R., Cadenas, C., Watzl, C., Nitsche, M.A., Kappenberg, F., Luedde, T., Longerich, T., Rahnenführer, J., Hoehme, S., Trauner, M., Hengstler, J.G., 2021. Spatio-temporal multiscale analysis of western diet-fed mice reveals a translationally relevant sequence of events during NAFLD progression. Cells 10, 2516. https://doi.org/10.3390/cells10102516.

Gómez-Lechón, M.J., Donato, M.T., Martínez-Romero, A., Jiménez, N., Castell, J.V., O'Connor, J.E., 2007. A human hepatocellular in vitro model to investigate steatosis. Chem. Biol. Interact. 165, 106–116. https://doi.org/10.1016/j.cbi.2006.11.004.

Greenspan, P., Mayer, E.P., Fowler, S.D., 1985. Nile red: a selective fluorescent stain for intracellular lipid droplets. J. Cell Biol. 100, 965–973. https://doi.org/10.1083/jcb.100.3.965.

Gu, X., Albrecht, W., Edlund, K., Kappenberg, F., Rahnenführer, J., Leist, M., Moritz, W., Godoy, P., Cadenas, C., Marchan, R., Brecklinghaus, T., Pardo, L.T., Castell, J.V., Gardner, I., Han, B., Hengstler, J.G., Stoeber, R., 2018. Relevance of the incubation period in cytotoxicity testing with primary human hepatocytes. Arch. Toxicol. 92, 3505–3515. https://doi.org/10.1007/s00204-018-2302-0.

Holland, C.H., Ramirez Flores, R.O., Myllys, M., Hassan, R., Edlund, K., Hofmann, U., Marchan, R., Cadenas, C., Reinders, J., Hoehme, S., Seddek, A. latif, Dooley, S., Keitel, V., Godoy, P., Begher-Tibbe, B., Trautwein, C., Rupp, C., Mueller, S.,

Longerich, T., Hengstler, J.G., Saez-Rodriguez, J., Ghallab, A., 2022. Transcriptomic cross-species analysis of chronic liver disease reveals consistent regulation between humans and mice. Hepatol. Commun. 6, 161–177. https://doi.org/10.1002/hep4.1797.

Hudert, C.A., Selinski, S., Rudolph, B., Bläker, H., Loddenkemper, C., Thielhorn, R., Berndt, N., Golka, K., Cadenas, C., Reinders, J., Henning, S., Bufler, P., Jansen, P.L. M., Holzhütter, H.G., Meierhofer, D., Hengstler, J.G., Wiegand, S., 2019. Genetic determinants of steatosis and fibrosis progression in paediatric non-alcoholic fatty liver disease. Liver Int. 39, 540–556. https://doi.org/10.1111/liv.14006.

Jaeschke, H., Gores, G.J., Cederbaum, A.I., Hinson, J.A., Pessayre, D., Lemasters, J.J., 2002. Mechanisms of hepatotoxicity. Toxicol. Sci. 65, 166–176. https://doi.org/10.1093/toxsci/65.2.166.

Khetani, S.R., Kanchagar, C., Ukairo, O., Krzyzewski, S., Moore, A., Shi, J., Aoyama, S., Aleo, M., Will, Y., 2013. Use of micropatterned cocultures to detect compounds that cause drug-induced liver injury in humans. Toxicol. Sci. 132, 107–117. https://doi.org/10.1093/toxsci/kfs326.

Kostrzewski, T., Cornforth, T., Snow, S.A., Ouro-Gnao, L., Rowe, C., Large, E.M., Hughes, D.J., 2017. Three-dimensional perfused human in vitro model of non-alcoholic fatty liver disease. World J. Gastroenterol. 23, 204–215. https://doi.org/10.3748/wjg.v23.i2.204.

Leist, M., Ghallab, A., Graepel, R., Marchan, R., Hassan, R., Bennekou, S.H., Limonciel, A., Vinken, M., Schildknecht, S., Waldmann, T., Danen, E., van Ravenzwaay, B., Kamp, H., Gardner, I., Godoy, P., Bois, F.Y., Braeuning, A., Reif, R., Oesch, F., Drasdo, D., Höhme, S., Schwarz, M., Hartung, T., Braunbeck, T., Beltman, J., Vrieling, H., Sanz, F., Forsby, A., Gadaleta, D., Fisher, C., Kelm, J., Fluri, D., Ecker, G., Zdrazil, B., Terron, A., Jennings, P., van der Burg, B., Dooley, S., Meijer, A.H., Willighagen, E., Martens, M., Evelo, C., Mombelli, E., Taboureau, O., Mantovani, A., Hardy, B., Koch, B., Escher, S., van Thriel, C., Cadenas, C., Kroese, D., van de Water, B., Hengstler, J.G., 2017. Adverse outcome pathways: opportunities, limitations and open questions. Arch. Toxicol. 91, 3477–3505. https://doi.org/10.1007/s00204-017-2045-3.

Levy, G., Cohen, M., Nahmias, Y., 2015. In vitro cell culture models of hepatic steatosis. Methods Mol. Biol. 1250, 377–390. https://doi.org/10.1007/978-1-4939-2074-7_29.

Mach, F., Ray, K.K., Wiklund, O., Corsini, A., Catapano, A.L., Bruckert, E., De Backer, G., Hegele, R.A., Hovingh, G.K., Jacobson, T.A., Krauss, R.M., Laufs, U., Leiter, L.A., März, W., Nordestgaard, B.G., Raal, F.J., Roden, M., Santos, R.D., Stein, E.A., Stroes, E.S., Thompson, P.D., Tokgözoglu, L., Vladutiu, G.D., Gencer, B., Stock, J.K., Ginsberg, H.N., Chapman, M.J., 2018. Adverse effects of statin therapy: perception vs. the evidence – focus on glucose homeostasis, cognitive, renal and hepatic function, haemorrhagic stroke and cataract. Eur. Heart J 39, 2526. https://doi.org/10.1093/EURHEARTJ/EHY182.

Malhi, H., Bronk, S.F., Werneburg, N.W., Gores, G.J., 2006. Free fatty acids induce JNK-dependent hepatocyte lipoapoptosis. J. Biol. Chem. 281, 12093–12101. https://doi.org/10.1074/jbc.M510660200.

Masubuchi, Y., 2006. Metabolic and non-metabolic factors determining troglitazone hepatotoxicity: a review. Drug Metab. Pharmacokinet. 21, 347–356. https://doi.org/10.2133/DMPK.21.347.

Matsubara, T., Li, F., Gonzalez, F.J., 2013. FXR signaling in the enterohepatic system. Mol. Cell. Endocrinol. 368, 17–29. https://doi.org/10.1016/J.MCE.2012.05.004.

Mohs, A., Otto, T., Schneider, K.M., Peltzer, M., Boekschoten, M., Holland, C.H., Hudert, C.A., Kalveram, L., Wiegand, S., Saez-Rodriguez, J., Longerich, T., Hengstler, J.G., Trautwein, C., 2021. Hepatocyte-specific NRF2 activation controls fibrogenesis and carcinogenesis in steatohepatitis. J. Hepatol. 74, 638–648. https://doi.org/10.1016/j.jhep.2020.09.037.

Müller, F.A., Sturla, S.J., 2019. Human in vitro models of nonalcoholic fatty liver disease. Curr. Opin. Toxicol. 16, 9–16. https://doi.org/10.1016/j.cotox.2019.03.001.

Padda, M.S., Sanchez, M., Akhtar, A.J., Boyer, J.L., 2011. Drug induced cholestasis. Hepatology 53, 1377. https://doi.org/10.1002/HEP.24229.

Pessayre, D., Fromenty, B., Berson, A., Robin, M.A., Lettéron, P., Moreau, R., Mansouri, A., 2012. Central role of mitochondria in drug-induced liver injury. Drug Metab. Rev. 44, 34–87. https://doi.org/10.3109/03602532.2011.604086.

Pillaye, J.N., Marakalala, M.J., Khumalo, N., Spearman, W., Ndlovu, H., 2020. Mechanistic insights into antiretroviral drug-induced liver injury. Pharmacol. Res. Perspect. 8, e00598 https://doi.org/10.1002/PRP2.598.

Proctor, W.R., Foster, A.J., Vogt, J., Summers, C., Middleton, B., Pilling, M.A., Shienson, D., Kijanska, M., Ströbel, S., Kelm, J.M., Morgan, P., Messner, S., Williams, D., 2017. Utility of spherical human liver microtissues for prediction of clinical drug-induced liver injury. Arch. Toxicol. 91, 2849–2863. https://doi.org/10.1007/s00204-017-2002-1.

Qu, B., Li, Q.T., Wong, K.P., Tan, T.M.C., Halliwell, B., 2001. Mechanism of clofibrate hepatotoxicity: mitochondrial damage and oxidative stress in hepatocytes. Free Radic. Biol. Med. 31, 659–669. https://doi.org/10.1016/S0891-5849(01)00632-3.

R. Core Team, 2021. A Language and Environment for Statistical Computing. R Found. Stat. Comput.

Raucy, J.L., Lasker, J., Ozaki, K., Zoleta, V., 2004. Regulation of CYP2E1 by ethanol and palmitic acid and CYP4A11 by clofibrate in primary cultures of human hepatocytes. Toxicol. Sci. 79, 233–241. https://doi.org/10.1093/TOXSCI/KFH126.

Ren, Z., Chen, S., Pak, S., Guo, L., 2021. A mechanism of perhexiline's cytotoxicity in hepatic cells involves endoplasmic reticulum stress and p38 signaling pathway. Chem. Biol. Interact. 334, 109353 https://doi.org/10.1016/J.CBI.2020.109353.

Ritz, C., Baty, F., Streibig, J.C., Gerhard, D., 2015. Dose-response analysis using R. PLoS One 10, e0146021. https://doi.org/10.1371/journal.pone.0146021.

Robin, X., Turck, N., Hainard, A., Tiberti, N., Lisacek, F., Sanchez, J.C., Müller, M., 2011. pROC: an open-source package for R and S+ to analyze and compare ROC curves. BMC Bioinform. 12, 1–8. https://doi.org/10.1186/1471-2105-12-77.

Sachinidis, A., Albrecht, W., Nell, P., Cherianidou, A., Hewitt, N.J., Edlund, K., Hengstler, J.G., 2019. Road map for development of stem cell-based alternative test methods. Trends Mol. Med. https://doi.org/10.1016/j.molmed.2019.04.003.

Schneider, K.M., Candels, L.S., Hov, J.R., Myllys, M., Hassan, R., Schneider, C.V., Wahlström, A., Mohs, A., Zühlke, S., Liao, L., Elfers, C., Kilic, K., Henricsson, M., Molinaro, A., Hatting, M., Zaza, A., Drasdo, D., Frissen, M., Devlin, A.S., Gálvez, E.J. C., Strowig, T., Karlsen, T.H., Hengstler, J.G., Marschall, H.U., Ghallab, A., Trautwein, C., 2021. Gut microbiota depletion exacerbates cholestatic liver injury via loss of FXR signalling. Nat. Metab. 3, 1228–1241. https://doi.org/10.1038/s42255-021-00452-1.

Scorletti, E., Carr, R.M., 2022. A new perspective on NAFLD: Focusing on lipid droplets. J. Hepatol. 76, 934–945. https://doi.org/10.1016/J.JHEP.2021.11.009.

Serras, A.S., Rodrigues, J.S., Cipriano, M., Rodrigues, A.V., Oliveira, N.G., Miranda, J.P., 2021. A critical perspective on 3D liver models for drug metabolism and toxicology studies. Front. Cell Dev. Biol. 9, 203. https://doi.org/10.3389/FCELL.2021.626805/BIBTEX.

Tolosa, L., Gómez-Lechón, M.J., Donato, M.T., 2017. A multi-parametric fluorescent assay for the screening and mechanistic study of drug-induced steatosis in liver cells in culture. Curr. Protoc. Toxicol. 2017, 1–11. https://doi.org/10.1002/cptx.20.

Vartak, N., Damle-Vartak, A., Richter, B., Dirsch, O., Dahmen, U., Hammad, S., Hengstler, J.G., 2016. Cholestasis-induced adaptive remodeling of interlobular bile ducts. Hepatology 63, 951–964. https://doi.org/10.1002/hep.28373.

Velsor, L.W., Kovacevic, M., Goldstein, M., Leitner, H.M., Lewis, W., Day, B.J., 2004. Mitochondrial oxidative stress in human hepatoma cells exposed to stavudine. Toxicol. Appl. Pharmacol. 199, 10–19. https://doi.org/10.1016/J.TAAP.2004.03.005.

Vorrink, S.U., Zhou, Y., Ingelman-Sundberg, M., Lauschke, V.M., 2018. Prediction of drug-induced hepatotoxicity using long-term stable primary hepatic 3D spheroid cultures in chemically defined conditions. Toxicol. Sci. 163, 655–665. https://doi.org/10.1093/TOXSCI/KFY058.

Weaver, R.J., Blomme, E.A., Chadwick, A.E., Copple, I.M., Gerets, H.H.J., Goldring, C.E., Guillouzo, A., Hewitt, P.G., Ingelman-Sundberg, M., Jensen, K.G., Juhila, S., Klingmüller, U., Labbe, G., Liguori, M.J., Lovatt, C.A., Morgan, P., Naisbitt, D.J., Pieters, R.H.H., Snoeys, J., van de Water, B., Williams, D.P., Park, B.K., 2020. Managing the challenge of drug-induced liver injury: a roadmap for the development and deployment of preclinical predictive models. Nat. Rev. Drug Discov. 19, 131–148. https://doi.org/10.1038/s41573-019-0048-x.

Westerink, W.M.A., Schoonen, W.G.E.J., 2007. Cytochrome P450 enzyme levels in HepG2 cells and cryopreserved primary human hepatocytes and their induction in HepG2 cells. Toxicol. Vitr. 21, 1581–1591. https://doi.org/10.1016/J.TIV.2007.05.014.

Winkler, I., Bitter, C., Winkler, S., Weichenhan, D., Thavamani, A., Hengstler, J.G., Borkham-Kamphorst, E., Kohlbacher, O., Plass, C., Geffers, R., Weiskirchen, R., Nordheim, A., 2020. Identification of Ppary-modulated miRNA hubs that target the fibrotic tumor microenvironment. Proc. Natl. Acad. Sci. U.S.A. 117, 454–463. https://doi.org/10.1073/pnas.1909145117.

Wu, C.Y., Benet, L.Z., 2005. Predicting drug disposition via application of BCS: Transport/absorption/ elimination interplay and development of a biopharmaceutics drug disposition classification system. Pharm. Res. 22, 11–23. https://doi.org/10.1007/s11095-004-9004-4.